

Eddy currents induced in a conducting rod of finite length by a coaxial encircling coil

This content has been downloaded from IOPscience. Please scroll down to see the full text.

2005 J. Phys. D: Appl. Phys. 38 2861

(<http://iopscience.iop.org/0022-3727/38/16/019>)

View [the table of contents for this issue](#), or go to the [journal homepage](#) for more

Download details:

IP Address: 128.149.47.225

This content was downloaded on 23/08/2016 at 20:16

Please note that [terms and conditions apply](#).

You may also be interested in:

[Eddy currents at a plate edge](#)

John R Bowler and Theodoros P Theodoulidis

[Impedance for solenoid coil](#)

Jing Wu and Yinzhao Lei

[Computation of a quasi-static field induced by two long straight parallel wires](#)

Denis Prémel

[Impedance of a horizontal coil in a borehole](#)

S K Burke and T P Theodoulidis

[A perturbation method for calculating coil impedance in eddy-current testing](#)

S K Burke

[Impedance of a horizontal coil above a conducting half-space](#)

S K Burke

[Determination of the thickness of copper coatings on steel](#)

Lennart Båvall

Eddy currents induced in a conducting rod of finite length by a coaxial encircling coil

John R Bowler¹ and Theodoros P Theodoulidis²

¹ Iowa State University, Center for Nondestructive Evaluation, Applied Sciences Complex II, 1915 Scholl Road, Ames IA 50011, USA

² Department of Engineering and Management of Energy Resources, University of West Macedonia, Kastorias and Fleming, 50100 Kozani, Greece

Received 18 February 2005, in final form 17 May 2005

Published 5 August 2005

Online at stacks.iop.org/JPhysD/38/2861

Abstract

This paper describes the calculation of eddy currents in a cylindrical conductive rod of finite length due to a coaxial circular coil carrying an alternating current. The coil impedance variation with frequency is determined from the field for an arbitrary coaxial location of the coil. Expressions for electromagnetic field and impedance of a coil encircling an infinite cylindrical rod are well known, the results being expressed as infinite integrals involving Bessel functions. For a finite length rod, additional boundary conditions must be satisfied at the ends. The extra boundary conditions are accommodated here by recasting the problem in a domain of finite extent in the axial direction. The axial length of the truncated domain is arbitrary and can be large compared with the coil length or the length of the rod. Therefore, the truncated domain solution can yield results that are numerically as close to the infinite domain solution as desired. The results provide a simple means of calculating the impedance of an inductor with a lossy core and can be used to investigate the linear properties of the core material.

(Some figures in this article are in colour only in the electronic version)

1. Introduction

The quasi-static electromagnetic field produced by a coil of rectangular cross-section coaxial with a infinitely long rod can be written in closed integral form [1, 2]. This useful solution has been applied to a number of problems in nondestructive evaluation [3–5]. Here we describe an analytical approach for calculating the quasi-static coil field in the presence of a coaxial rod of finite length taking the end effects into account.

In general, the field inside a finite rod having linear material properties should be appropriately matched at the interface with the field in the surrounding medium, assumed here to be nonconductive. In the case of an infinite rod, the interface conditions are applied at its cylindrical surface only, but for a finite rod, they must also be applied at its ends. Special solutions for the field excited by a coaxial coil encircling a finite rod have been found in this manner for the case where the coil current has even symmetry about the rod mid-plane,

perpendicular to the axis. Both time harmonic and transient solutions have been determined [6].

An analytical result for a similar even source problem was later found on the assumption that the relative permeability of the rod is very much greater than one. This assumption implies that the axial magnetic field, H_z , within, and at a point approaching the end of the rod can be approximated as zero [7]. The approximation provides a convenient boundary condition at the circular ends of the rod for the solution representing the internal field. However, since the solution sought is supposed to represent the field of a finite length ferrite rod in free space, it should not constrain H_z , to be zero over the whole of the surfaces coplanar with the rod ends, but unfortunately, this is what the authors have done.

Here, we determine the quasi-static field of a cylindrical coil of rectangular cross-section whose centre is at an arbitrary location on the axis of a finite length conductive rod (figure 1). The solution is a generalization of that given by Nethe [6] and

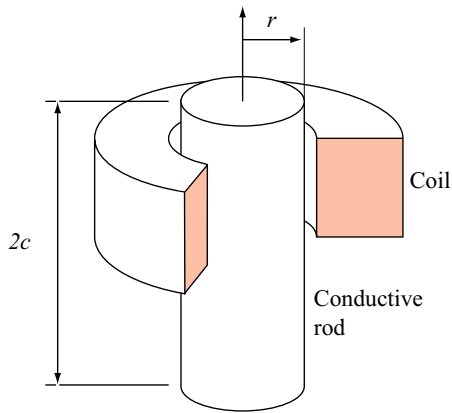


Figure 1. Coil encircling a finite cylindrical rod, length $2c$ radius r .

uses a similar method, but is not confined to the even source case. The procedure, based on mode matching in a truncated domain, is easily adapted to deal with a finite layered rod or a finite tube. A similar analysis has previously been given to account for the end effects produced by an internal bobbin coil in a finite coaxial cylindrical tube [8]. The procedure has also been used to study a ferrite-cored eddy current probe [9] and a coil coaxial with a hole in a plate [10].

2. Magnetic vector potential

Consider a time-harmonic field varying in time t at an angular frequency ω as the real part of $\exp(-i\omega t)$. The electric and magnetic field due to a coil encircling a conducting cylinder can be written in terms of the magnetic vector potential $\mathbf{A} = \hat{\phi}A$ as

$$E_\phi = i\omega A \quad \text{and} \quad \mathbf{H} = \frac{1}{\mu_0\mu_r} \nabla \times (\hat{\phi}A), \quad (1)$$

where μ_r is the relative permeability. The vector potential satisfies

$$\nabla^2 \mathbf{A} = -\mu_0 \mathbf{J} \quad (2)$$

in the region outside the conductor, where $\mathbf{J} = J_\phi \hat{\phi}$ is the current density of the source coil. The magnetic vector potential for the conductive region satisfies the homogeneous Helmholtz equation

$$(\nabla^2 + k^2)\mathbf{A} = 0 \quad (3)$$

subject to interface conditions ensuring that the tangential electric and magnetic fields are continuous at the surface of the conductor. In (3), $k^2 = i\omega\mu_0\mu_r\sigma$, where σ is the electrical conductivity of the rod.

For an axially symmetric field, separation of variables requires that a solution is sought in the form of a product of two functions, say $R(\rho)$ and $Z(z)$. Setting $(d^2Z/dz^2)/Z = -\kappa^2$ leads to a solution for the conductive region of the form

$$Z(z) = a(\kappa) \sin(\kappa z) + b(\kappa) \cos(\kappa z), \quad (4)$$

$$R(\rho) = C(\kappa)I_1(\gamma\rho) + D(\kappa)K_1(\gamma\rho), \quad (5)$$

where $\gamma = (\kappa^2 - i\omega\mu_0\mu_r\sigma)^{1/2}$, taking the root with a positive real part. One of the functions $a(\kappa)$, $b(\kappa)$, $C(\kappa)$ and $D(\kappa)$ is

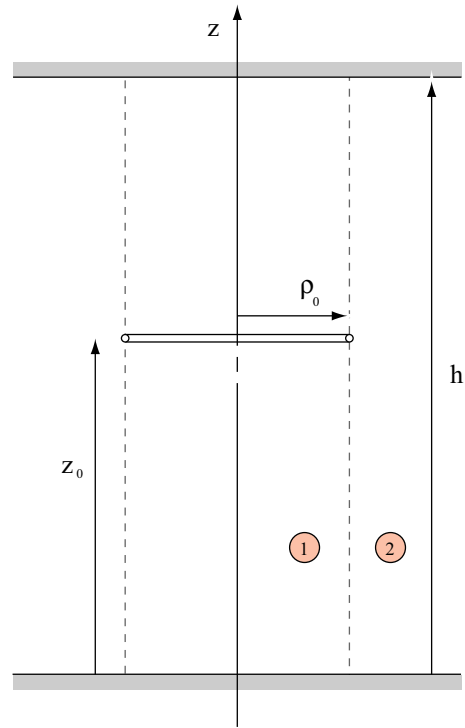


Figure 2. Circular current filament in a truncated domain.

redundant, $D(\kappa)$ is zero because otherwise the $K_1(\gamma\rho)$ would give a singular field on the axis and the other two unknown functions of κ are determined by the interface conditions.

For the nonconducting region, one can either replace γ in the Bessel function arguments of (5) with κ to get a solution or replace κ in the trigonometric function argument of (4) with γ . In either case, (2) is satisfied, except in the source region. The latter option is used for the nonconducting region adjacent to the end of the rod, ensuring that the radial solution for the nonconducting region matches that for the conductive region across the ends of the rod.

3. Current source field

A general solution for an infinite rod is expressed in terms of integrals of the product $R(\rho)Z(z)$ with respect to κ over the range zero to infinity. However, in order to calculate a solution for a finite rod, it is helpful to truncate the domain of the problem in the z -direction to a zone bounded at $z = -h$ and h . Then the field is expressed as a summation, rather than as an integral. Only half of this domain is considered (figure 2), since the required solution is a linear combination of solutions that are odd and even in z . A solution for the truncated domain is not identical to one for the infinite domain, but by making h as large as necessary, it is possible, in principle, to make the numerical results for the truncated domain as close as desired to the unbounded domain results.

The development here is in three steps. First, a filamentary coil solution is established for the truncated domain. Next, the filament solutions are superimposed to get a coil solution and finally the effects of the finite coaxial rod are included. It will be assumed that the tangential electric field on the boundary

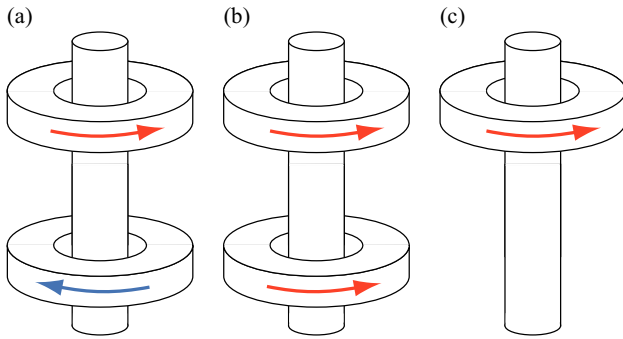


Figure 3. The parity of the solution, with respect to the z variable is defined here in terms of the coil current. (a) Odd parity configuration in which two identical coils symmetrically placed about the plane $z = 0$ carry current in opposite directions. (b) Even parity configuration in which the current is in the same direction. (c) The field of a single coil is half the sum of the odd or even solutions.

$z = h$ is zero. Initially, the solution sought for A is one which has odd symmetry with respect to z : $A(\rho, z) = -A(\rho, -z)$. A solution for even symmetry is also given following a similar procedure.

3.1. Symmetry

The odd parity solution represents the field due to a rod length $2h$ encircled by two identical coaxial coils carrying current in the opposite azimuthal directions and located symmetrically on opposite sides of the $z = 0$ plane, figure 3. If the rod happens to be long and the coils well separated then the electric field due to one such coil may be negligible in the $z = 0$ plane, in which case, the odd parity solution gives a good approximation to the field of a single coil in the half-space that it occupies. It should also give a good approximation to the problem of a coil on a semi-infinite rod since, for example, the location of the end of the rod in the negative- z half-space would have a negligible effect on the field in the positive- z half-space.

In order to represent end effects due to a short rod and a co-axial coil, both odd and even parity solutions are needed. The even parity solution represents the field due to two identical coaxial coils carrying current in the same azimuthal direction symmetrically placed about the $z = 0$ plane, figure 3. Incidentally, if the rod is long and the coils well separated, even and odd solutions should be similar in one half-space, for $z > 0$, say. Half the sum of the odd and even solutions gives the solution for one coil encircling a finite rod of arbitrary length.

3.2. Filament field of odd parity

The current density of a filament, expressed in terms of the current I is

$$J_\phi = I\delta(z - z_0)\delta(\rho - \rho_0) \quad (6)$$

and the magnetic vector potential due to the filament is $\mu_0 I \mathbf{G}$ where $\mathbf{G} = G\hat{\phi}$ satisfies

$$\nabla^2 \mathbf{G}(\rho, z|\rho_0, z_0) = -\delta(\rho - \rho_0)\delta(z - z_0)\hat{\phi}. \quad (7)$$

Putting $G = G_1$ for the region 1 solution, and $G = G_2$ for the region 2 solution, figure 2, the solution of (7) is written as

$$G_1(\rho, z|\rho_0, z_0) = \sum_j \sin(\kappa_j z) I_1(\kappa_j \rho) c_j^{(0)}(\rho_0, z_0), \quad (8)$$

which must remain finite at the axis with

$$G_2(\rho, z|\rho_0, z_0) = \sum_j \sin(\kappa_j z) K_1(\kappa_j \rho) d_j^{(0)}(\rho_0, z_0), \quad (9)$$

which vanishes as $\rho \rightarrow \infty$, and where $\kappa_j = j\pi/h$ with $j = 1, 2, 3, \dots$. Although the solution is expressed here as an infinite sum, for numerical calculations a finite number of terms is taken.

The continuity conditions at the interface of region 1 and 2 are

$$G_1 = G_2 \quad \text{and} \quad \left. \frac{\partial G_1}{\partial \rho} \right|_{\rho=\rho_0} = \left. \frac{\partial G_2}{\partial \rho} \right|_{\rho=\rho_0} + \delta(z - z_0). \quad (10)$$

This second condition is found by integrating (7) between $\rho_0 - \epsilon$ and $\rho_0 + \epsilon$, and taking the limit as ϵ tends to zero. Substituting (8) and (9) into (10) and multiplying by $\sin(\kappa_i z)$, integrating with respect to z between 0 and h and using the orthogonality property,

$$\int_0^h \sin\left(\frac{n\pi x}{h}\right) \sin\left(\frac{m\pi x}{h}\right) dx = \frac{h}{2} \delta_{nm}, \quad (11)$$

gives

$$I_1(\kappa_j \rho_0) c_j^{(0)}(\rho_0, z_0) = K_1(\kappa_j \rho_0) d_j^{(0)}(\rho_0, z_0) \quad (12)$$

and

$$\left. \frac{\partial I_1(\kappa_j \rho)}{\partial \rho} \right|_{\rho=\rho_0} c_j^{(0)}(\rho_0, z_0) = \left. \frac{\partial K_1(\kappa_j \rho)}{\partial \rho} \right|_{\rho=\rho_0} d_j^{(0)}(\rho_0, z_0) + \frac{2}{h} \sin(\kappa_j z_0), \quad (13)$$

from which it is found, using expressions for the derivatives and the Wronskian of associated Bessel functions [13]³, that

$$c_j^{(0)}(\rho_0, z_0) = \frac{2}{h} \sin(\kappa_j z_0) \rho_0 K_1(\kappa_j \rho_0) \quad (14)$$

and

$$d_j^{(0)}(\rho_0, z_0) = \frac{2}{h} \sin(\kappa_j z_0) \rho_0 I_1(\kappa_j \rho_0). \quad (15)$$

The filament field is thus given by (8) and (9) with the expansion coefficient found from (14) and (15). Note that the field due to a coaxial coil with an arbitrary cross-section can be determined from a superposition of filament fields and likewise, the field of more than one coaxial coil, possibly configured differentially, may be found by applying the superposition principle.

3.3. Coil field

In general, the vector potential for an axially symmetric coil is given by a superposition of filament fields expressed as

$$A(\rho, z) = \mu_0 \int_{S_c} G(\rho, z|\rho_0, z_0) J_\phi(\rho_0, z_0) dS, \quad (16)$$

where S_c is the coil cross-section. The vector potential in region 2 due to the coil, figure 4 has the form

$$A_2(\rho, z) = \mu_0 n_d I \sum_j \sin(\kappa_j z) I_1(\kappa_j \rho) C_j^{(0)}. \quad (17)$$

³ Derivative of associated Bessel functions are given by 9.6.26 and we use the Wronskian 9.6.15.

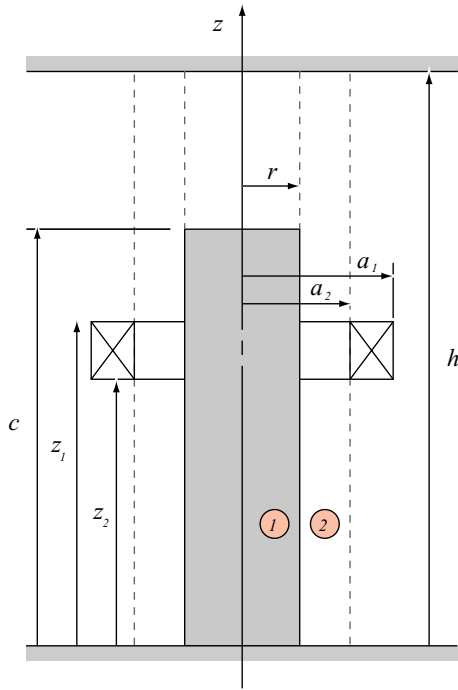


Figure 4. Coil coaxial with a finite rod.

For a tightly-wound uniform coil of rectangular cross-section, one writes the current density as $n_d I$, where n_d is the coil turns density. Substituting (8) into (16), integrating over the coil cross-section and comparing the resultant relationship with (17) gives

$$C_j^{(0)} = \int_{a_2}^{a_1} \int_{z_2}^{z_1} c_j^{(0)}(\rho_0, z_0) d\rho_0 dz_0$$

$$= -\frac{2}{h\kappa_j^3} [\cos(\kappa_j z_1) - \cos(\kappa_j z_2)] \mathcal{K}_1(\kappa_j a_1, \kappa_j a_2), \quad (18)$$

where

$$\mathcal{K}_1(r_1, r_2) = \int_{r_2}^{r_1} r K_1(r) dr, \quad (19)$$

which can be expressed in terms of a Meijer G -function, or in terms of Struve and Bessel functions [12].

4. Rod field

The above analysis can be extended to the case where the coil encircles a finite conductive rod, radius r (figure 4), by writing the odd parity solution as

$$A_1(\rho, z) = \mu_0 n_d I \sum_j \left[\frac{\sin(q_j z)}{\alpha_j \sin[\gamma_j(h-z)]} \right] I_1(\gamma_j \rho) C_j$$

$$0 \leq z < c, \quad (20)$$

$$c \leq z \leq h,$$

$$A_2(\rho, z) = \mu_0 n_d I \sum_j \sin(\kappa_j z) [I_1(\kappa_j \rho) C_j^{(0)} + K_1(\kappa_j \rho) D_j]$$

$$0 \leq z < h, \quad (21)$$

where $\kappa_j = j\pi/h$ and $C_j^{(0)}$ is given by (18) from the analysis of the coil in free space. The eigenvalues γ_j and q_j are related

by $\gamma_j = \sqrt{q_j^2 - i\omega\mu_0\mu_r\sigma}$ and are found as follows. Using the continuity of H_ρ at the end of the rod, it is found from equation (20) that

$$\alpha_j = -\frac{q_j \cos(q_j c)}{\mu_r \gamma_j \cos[\gamma_j(h-c)]} \quad (22)$$

and from the continuity of E_ϕ at the end of the rod,

$$\sin(q_j c) = \alpha_j \sin[\gamma_j(h-c)]. \quad (23)$$

With α_j given by (22), the values of q_j are sought which satisfy

$$\mu_r \gamma_j \tan(q_j c) + q_j \tan[\gamma_j(h-c)] = 0, \quad (24)$$

which is found from (22) and (23).

From the continuity of E_ϕ and H_z at $\rho = r$,

$$A_1 = A_2 \quad (25)$$

and

$$\begin{bmatrix} 1 \\ \mu_r \\ 1 \end{bmatrix} \frac{1}{r} \frac{\partial(\rho A_1)}{\partial \rho} \Big|_{\rho=r} = \begin{bmatrix} 1 \\ 1 \end{bmatrix} \frac{1}{r} \frac{\partial(\rho A_2)}{\partial \rho} \Big|_{\rho=r} \quad \begin{matrix} 0 \leq z < c, \\ c \leq z \leq h. \end{matrix} \quad (26)$$

Substituting (20) and (21) into (25), multiplying by $\sin(\kappa_i z)$ and integrating from zero to h gives

$$U I_1(\gamma r) C = I_1(\kappa r) C^{(0)} + K_1(\kappa r) D. \quad (27)$$

Similarly, from (26),

$$\frac{1}{\mu_r} V I_0(\gamma r) \gamma C = I_0(\kappa r) \kappa C^{(0)} - K_0(\kappa r) \kappa D. \quad (28)$$

Here Bessel functions with bold symbol arguments represent diagonal matrices. $C^{(0)}$, C and D are column vectors of expansion coefficients. U and V are matrices whose elements are given by

$$U_{ij} = \frac{2}{h} \left[\int_0^c \sin(\kappa_i z) \sin(q_j z) dz - \frac{q_j \cos(q_j c)}{\mu_r \gamma_j \cos[\gamma_j(h-c)]} \int_c^h \sin(\kappa_i z) \sin[\gamma_j(h-z)] dz \right] \quad (29)$$

and

$$V_{ij} = \frac{2}{h} \left[\int_0^c \sin(\kappa_i z) \sin(q_j z) dz - \frac{q_j \cos(q_j c)}{\gamma_j \cos[\gamma_j(h-c)]} \int_c^h \sin(\kappa_i z) \sin[\gamma_j(h-z)] dz \right]. \quad (30)$$

The first integral in (29) and (30) is calculated from

$$\int_0^c \sin(\kappa_i z) \sin(q_j z) dz = \begin{cases} \frac{\sin[(q_j - \kappa_i)c]}{2(q_j - \kappa_i)} - \frac{\sin[(q_j + \kappa_i)c]}{2(q_j + \kappa_i)}, & \kappa_i \neq q_j, \\ \frac{c}{2} - \frac{\sin(2\kappa_i c)}{4\kappa_i}, & \kappa_i = q_j \end{cases} \quad (31)$$

and the second, from

$$\int_c^h \sin(\kappa_i z) \sin[\gamma_j (h - z)] dz = \begin{cases} (\kappa_i \cos(\kappa_i c) \sin[\gamma_j (c - h)] - \gamma_j \sin(\kappa_i c) \\ \quad \times \cos[\gamma_j (c - h)]) (\gamma_j^2 - \kappa_i^2)^{-1}, & \kappa_i \neq \gamma_j, \\ (2(c - h) \kappa_i \cos(\kappa_i h) \\ \quad + \sin[\kappa_i (h - 2c)]) (4\kappa_i)^{-1}, & \kappa_i = \gamma_j. \end{cases} \quad (32)$$

Eliminate \mathbf{D} by adding $K_0(\kappa r) \kappa \times (27)$ to $K_1(\kappa r) \times (28)$ to give

$$\mathbf{C} = \frac{1}{r} \left[K_0(\kappa r) \kappa \mathbf{U} I_1(\gamma r) + \frac{K_1(\kappa r) \mathbf{V} I_0(\gamma r) \gamma}{\mu_r} \right]^{-1} \mathbf{C}^{(0)}. \quad (33)$$

Similarly, eliminate $\mathbf{C}^{(0)}$ by subtracting $I_1(\kappa r) \times (28)$ from $I_0(\kappa r) \kappa \times (27)$ to give

$$\mathbf{D} = r \left[I_0(\kappa r) \kappa \mathbf{U} I_1(\gamma r) - \frac{I_1(\kappa r) \mathbf{V} I_0(\gamma r) \gamma}{\mu_r} \right] \mathbf{C}. \quad (34)$$

Combining (33) and (34) gives

$$\mathbf{D} = \mathbf{W} \mathbf{C}^{(0)}, \quad (35)$$

where

$$\mathbf{W} = \left[I_0(\kappa r) \kappa \mathbf{U} I_1(\gamma r) - \frac{I_1(\kappa r) \mathbf{V} I_0(\gamma r) \gamma}{\mu_r} \right] \times \left[K_0(\kappa r) \kappa \mathbf{U} I_1(\gamma r) + \frac{K_1(\kappa r) \mathbf{V} I_0(\gamma r) \gamma}{\mu_r} \right]^{-1}. \quad (36)$$

Equations (33) and (34) give the coefficients in (20) and (21) in terms of the prescribed source coefficients $\mathbf{C}^{(0)}$ defined by (18).

5. Even parity solution

The even parity solution can be found following a procedure similar to that given in the foregoing sections for the odd parity solution. Rather than going through the derivation in full, the distinctive features of the even parity solution are summarized below. It is worth noting at the outset, however, that the main results of the previous section, equations (33)–(36) can be preserved in their original form to represent either odd, even or a linear combination of both odd and even solutions. One only needs to introduce a new set of eigenvalues for κ and q , and modifying the definition of the matrices, \mathbf{U} and \mathbf{V} the one-coil solution is obtained. These modifications will now be outlined.

Consider first, the fundamental solutions, (8) and (9). For the even solution, these must be expressed in terms of cosines rather than sines of κz . Consequently, the condition that the field vanishes at the boundary $z = h$ is satisfied by letting $\kappa_j = (2j - 1)\pi/2h$, $j = 1, 2, 3, \dots$. Then, instead of (18), the coefficients $C_j^{(0)}$, for the even solution are given by

$$C_j^{(0)} = \frac{2}{h\kappa_j^3} [\sin(\kappa_j z_1) - \sin(\kappa_j z_2)] \mathcal{K}_1(\kappa_j a_1, \kappa_j a_2). \quad (37)$$

With the expression in (20) for the vector potential representing the field in the region 1 replaced by

$$A_1(\rho, z) = \mu_0 n_d I \sum_j \left[\begin{array}{c} \cos(q_j z) \\ \alpha_j \sin[\gamma_j (h - z)] \end{array} \right] I_1(\gamma_j \rho) C_j, \quad \begin{array}{l} 0 \leq z < c, \\ c \leq z \leq h \end{array} \quad (38)$$

and with (21) rewritten with the cosine in place of the sine, it is found from the continuity conditions at the end of the rod, that the new eigenvalues for the even symmetry case are solutions of

$$q_j \tan(q_j c) - \mu_r \gamma_j \cot[\gamma_j (h - c)] = 0. \quad (39)$$

Finally, it is found that the matrices \mathbf{U} and \mathbf{V} are defined in terms of the new appropriate eigenvalues for an even solution with their matrix elements, given by

$$U_{ij} = \frac{2}{h} \left[\int_0^c \cos(\kappa_i z) \cos(q_j z) dz + \frac{\cos(q_j c)}{\sin[\gamma_j (h - c)]} \times \int_c^h \cos(\kappa_i z) \sin[\gamma_j (h - z)] dz \right] \quad (40)$$

and

$$V_{ij} = \frac{2}{h} \left[\int_0^c \cos(\kappa_i z) \cos(q_j z) dz + \frac{\mu_r \cos(q_j c)}{\sin[\gamma_j (h - c)]} \times \int_c^h \cos(\kappa_i z) \sin[\gamma_j (h - z)] dz \right]. \quad (41)$$

The first integral in (40) and (41) is calculated from

$$\int_0^c \cos(\kappa_i z) \cos(q_j z) dz = \begin{cases} \frac{\sin[(q_j - \kappa_i)c]}{2(q_j - \kappa_i)} + \frac{\sin[(q_j + \kappa_i)c]}{2(q_j + \kappa_i)}, & \kappa_i \neq q_j, \\ \frac{c}{2} + \frac{\sin(2c\kappa_i)}{4\kappa_i}, & \kappa_i = q_j \end{cases} \quad (42)$$

and the second, from

$$\int_c^h \cos(\kappa_i z) \sin[\gamma_j (h - z)] dz = \begin{cases} (-\kappa_i \sin(\kappa_i c) \sin[\gamma_j (c - h)] - \gamma_j \cos(\kappa_i c) \\ \quad \times \cos[\gamma_j (c - h)]) (\gamma_j^2 - \kappa_i^2)^{-1}, & \kappa_i \neq \gamma_j, \\ (2(h - c) \kappa_i \sin(\kappa_i h) \\ \quad - \cos[\kappa_i (h - 2c)]) (4\kappa_i)^{-1}, & \kappa_i = \gamma_j. \end{cases} \quad (43)$$

6. Impedance

The impedance can be calculated from a relationship derived using a reciprocity theorem [14]:

$$I^2 \Delta Z = \int_{S_0} (\Delta \mathbf{E} \times \mathbf{H}^{(0)} - \mathbf{E}^{(0)} \times \Delta \mathbf{H}) \cdot d\mathbf{S}, \quad (44)$$

where the superscript (0) indicates the field in the absence of the conducting rod. $\Delta \mathbf{E}$ and $\Delta \mathbf{H}$ are the electric and magnetic field due to the presence of the rod. The surface S_0 encloses the primary source, the coil in this case, and the direction of $d\mathbf{S}$ is that of an outward normal with respect to the source.

The surface S_0 will be taken to be in the region at the surface of radius a . Substituting the vector potential into the equation for the impedance due to the rod gives

$$I^2 \Delta Z = \frac{2\pi i \omega}{\mu_0} \int_0^h \left[A^{(0)} \frac{\partial(\rho \Delta A)}{\partial \rho} - \Delta A \frac{\partial(\rho A^{(0)})}{\partial \rho} \right]_{\rho=a} dz. \quad (45)$$

Using (20) and (21) and applying Parseval's theorem for Fourier series, one finds that

$$\Delta Z = -i \omega \mu_0 \pi h n_d^2 \mathbf{C}^{(0)} \mathbf{W} \mathbf{C}^{(0)}. \quad (46)$$

This expression is valid for both, the odd and even parity solutions. We just have to use the appropriate vector $\mathbf{C}^{(0)}$, matrices \mathbf{U} and \mathbf{V} and eigenvalues κ and γ for each parity. The final impedance change is computed via the average of the even and odd parity fields.

7. Corroboration

A useful check on the formulation can be done by considering the limiting case $c \rightarrow h$ when the solution represents the case of a coil encircling an infinitely long rod. In this case, all of the matrices are diagonal and the final expression for the impedance change can be given in the form of a series. The following simplified expressions are deduced after considering (46) for the odd or even parity solutions in the limit of $c \rightarrow h$.

$$\Delta Z = i \omega \mu_0 \pi h n_d^2 \sum_j [C_j^{(0)}]^2 \times \frac{\kappa_j \mu_r I_0(\kappa_j r) I_1(\gamma_j r) - \gamma_j I_1(\kappa_j r) I_0(\gamma_j r)}{\kappa_j \mu_r K_0(\kappa_j r) I_1(\gamma_j r) + \gamma_j K_1(\kappa_j r) I_0(\gamma_j r)}. \quad (47)$$

The coil can be placed at various positions in this limiting case. If it is placed at $z = 0$ we need to consider only the even parity solution. We can also put the coil at the middle of the half geometry at $c = h/2$. While the impedance change should, in principle, be based again on calculating the average of the odd and even parity solutions, we can get an approximate solution by taking into account only one of them. Equation (47) can be compared to the classical integral expression derived in [2]

$$\Delta Z = i \omega \mu_0 4n_d^2 \int_0^\infty \mathcal{K}_1(\kappa a_1, \kappa a_2)^2 \frac{1 - \cos[\kappa(z_2 - z_1)]}{\kappa^6} \times \frac{\kappa \mu_r I_0(\kappa r) I_1(\gamma r) - \gamma I_1(\kappa r) I_0(\gamma r)}{\kappa \mu_r K_0(\kappa r) I_1(\gamma r) + \gamma K_1(\kappa r) I_0(\gamma r)} d\kappa. \quad (48)$$

For the finite length rod, the most important numerical aspect of the presented formulation is the calculation of eigenvalues. A detailed analysis of the Newtonian iteration process used in finding the complex roots of (24) and (39) is described elsewhere [11]. In the same reference, we provide a rule of thumb on the number of required eigenvalues and the extent of the truncated region h . We base our selection on the use of these quantities in the case of the long rod and on the comparison of (47) and (48). For a larger solution domain, a greater number of eigenfunctions is needed to achieve accurate results. However, the larger domain more accurately approximates the infinite domain problem.

Apart from the calculation of eigenvalues, the other significant numerical aspect of the solution is the inversion

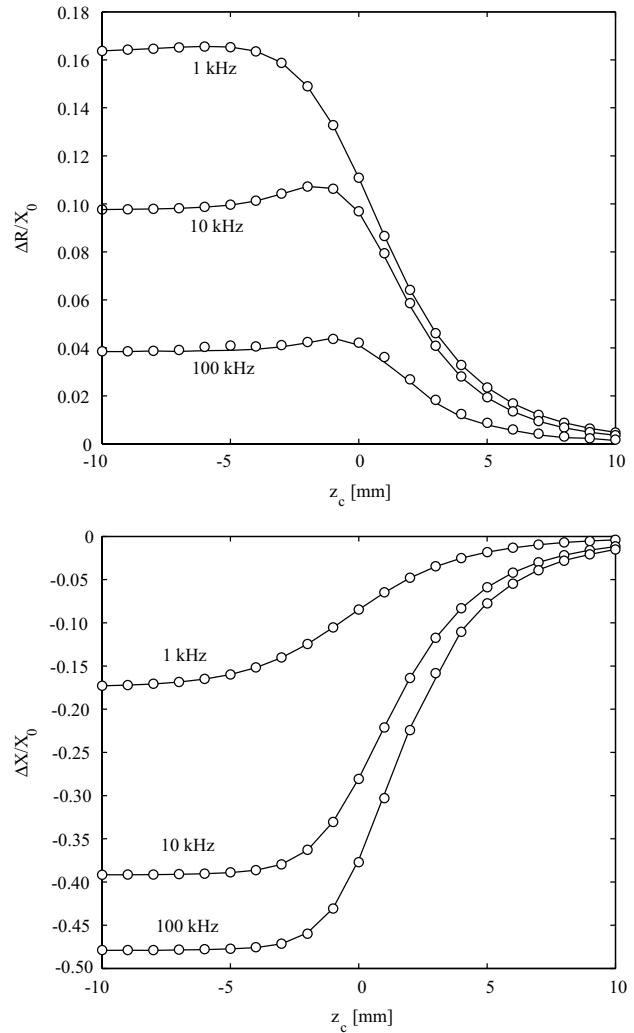


Figure 5. Variation of coil resistance and reactance change with distance from the rod end: comparison between results of eigenfunction expansions (—) and a finite element calculation (○ ○ ○ ○ ○).

of the full matrix in (36), which is a rather trivial task when using either a higher programming language or a general mathematical package such as Mathematica or Matlab. Let us only emphasize that in a parametric study involving the rod radius or the position and dimensions of the coil, this matrix needs to be inverted only once. In situations like this, the method is advantageous over other numerical methods such as the finite element method (FEM). For example, for one coil position the CPU times of eigenfunction expansions and the FEM are about the same, with most of the time in the eigenfunction expansions method spent on the computation of eigenvalues. For more coil positions, however, the method is much faster since the matrix inversion and computation of eigenvalues do not need to be repeated. The number of coil positions is a rough estimate of how many times the method is faster than the FEM.

In the following, we show the calculated impedance variation of a coil as it is traversed across the end of a semi-infinite rod. This geometry actually simulates the end effect in terms of an impedance variation and is modelled here by setting $c = h/2$. Figure 5 shows the coil resistance and reactance

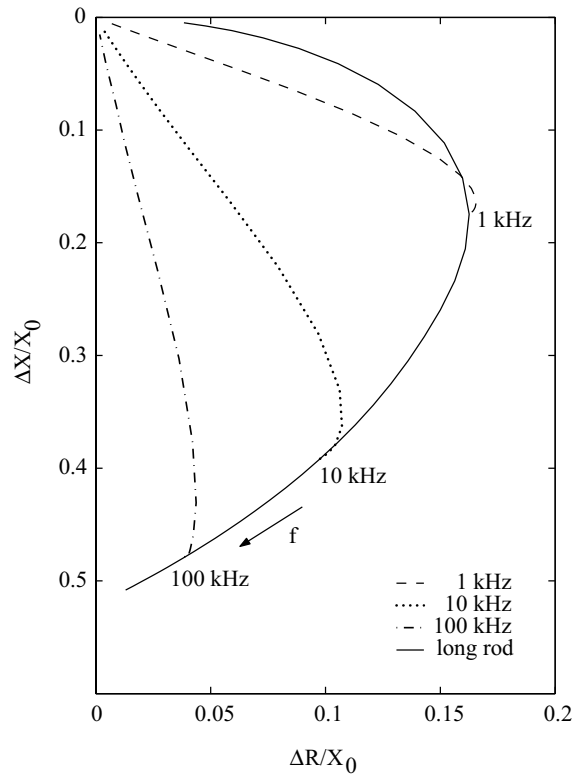


Figure 6. Normalized impedance plane showing the variation of the coil impedance with frequency for a long rod (—). Note that the direction of increasing frequency is indicated by the arrow. The variation of the coil impedance with distance z_c , from the rod end is shown by the dashed lines for three different frequencies.

changes at three distinct frequencies when the coil is traversed across the end of an aluminum rod. The rod conductivity is 18.72 MS m^{-1} . The coil parameters are $a_1 = 10 \text{ mm}$, $a_2 = 9 \text{ mm}$, $z_1 - z_2 = 4 \text{ mm}$ and $N = 400$. The solution domain length is $h = 200 \text{ mm}$ and the number of terms in the series is $N_s = 80$. For the limiting case of an infinite rod, these values of h and N_s gave an agreement with the integral expression, to within 0.1% for all frequencies. The ordinate $z_c = (z_2 + z_1)/2 - c$ denotes the distance of the coil centre from the rod end, and is negative when the coil encircles the rod. The impedance change is normalized, the normalization factor being the isolated coil reactance X_0 [1]. The theoretical results are compared with the numerical ones obtained with a two-dimensional finite element package and excellent agreement is obtained. The same information is also shown in figure 6 as an impedance plane diagram, together with the frequency curve of the same coil encircling an infinitely long rod. The significant feature of these results is that, while the coil reactance increases monotonically as the coil is traversed across the end, the resistance peaks before decreasing, a behaviour which was also observed in [8].

Next, we depict the effect of the aluminum rod length on the impedance change of the encircling coil when it is placed at the centre of the rod. The results in figure 7 show that the rod length starts to have a noticeable effect on the coil impedance when it is smaller than two coil lengths with the stronger relative change taking place at lower frequencies. Note that ultimately the coil resistance changes at 10 and 100 kHz will

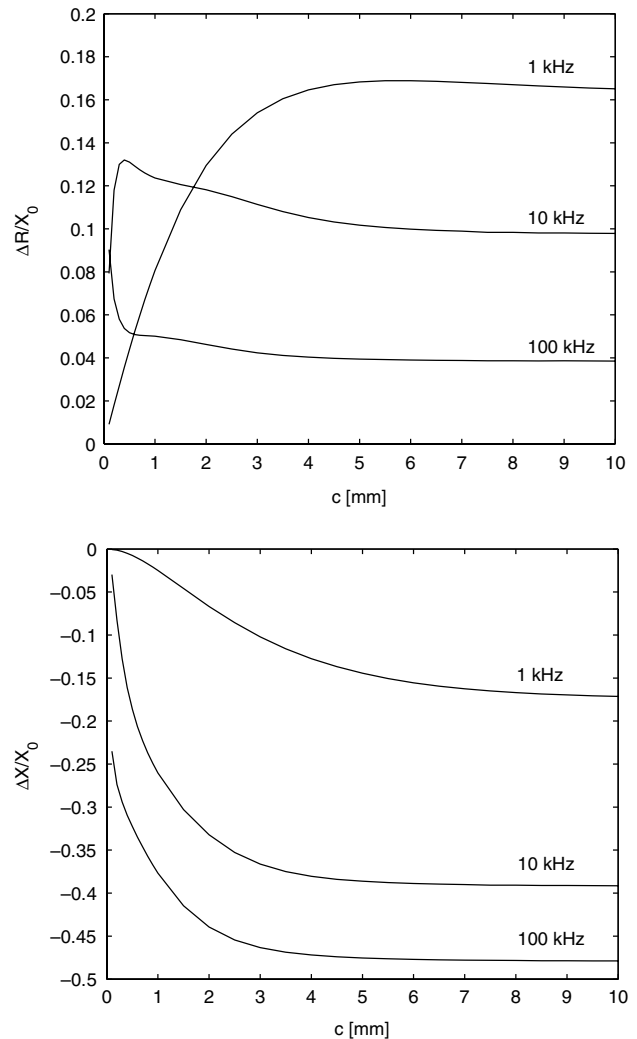


Figure 7. Variation of coil resistance and reactance change with rod length.

also decrease to zero, but this happens for a rod length which is much smaller than 1 mm.

8. Conclusion

The axisymmetric problem of a coil encircling a finite length rod was solved in this paper using eigenfunction expansions. The method has numerical aspects such as the inversion of a full matrix and the computation of eigenvalues but it avoids the discretization of the solution domain and yields analytical expressions in closed form.

The eigenfunction expansions method is a very useful tool since it has the power to solve many important eddy current problems. Possible extensions and potential applications of the method include analysis of a layered rod or a finite length tube or a rod with axisymmetric grooves.

Acknowledgment

This work was supported by the NSF/IU Program at CNDE, Iowa State University.

References

- [1] Dodd C V and Deeds W E 1968 *J. Appl. Phys.* **39** 2829
- [2] Dodd C V, Deeds W E and Luquire J W 1969 *Int. J. Nondestr. Test.* **1** 29
- [3] Grimberg R, Radu E, Savin A and Chifan S 1999 *J. Phys. D: Appl. Phys.* **32** 832
- [4] Uzal E, Ozkol I and Kaya M O 1998 *IEEE Trans. Mag.* **34** 213
- [5] deHalleux B and Ptchelintsev A 1997 *Insight* **39** 854
- [6] Nethe A 1991 *Arch. Elektrotech.* **74** 389
- [7] Wu J and Lei Y 2002 *J. Phys. D: Appl. Phys.* **35** 570
- [8] Theodoulidis T P 2003 *Int. J. Appl. Electromagn. Mech.* **18** 1
- [9] Theodoulidis T P 2003 *J. Appl. Phys.* **93** 3071
- [10] Theodoulidis T P and Bowler J R 2005 *Review of Progress in Quantitative Nondestructive Evaluation* vol 24 (New York: AIP) p 403
- [11] Theodoulidis T P and Bowler J R 2005 *IEEE Trans. Mag.* **41** 1238
- [12] Gradshteyn I S and Ryzhik I M 1980 *Tables of Integrals Series and Products*, 6.561 (New York: Academic)
- [13] Abramowitz M and Stegun I A 1970 *Handbook of Mathematical Functions with Formulas (Graphs and Mathematical Tables)* (New York: Wiley)
- [14] Auld B A and Moulder J C 1999 *J. Nondestruc. Eval.* **18** 3